

## Isothiocyanate iberin modulates phase II enzymes, posttranslational modification of histones and inhibits growth of Caco-2 cells by inducing apoptosis\*

J. JAKUBIKOVA<sup>1,2</sup>, Y. BAO<sup>2,3</sup>, J. BODO<sup>1</sup>, J. SEDLAK<sup>1\*\*</sup>

<sup>1</sup>Laboratory of Tumor Immunology, e-mail: exonsedl@savba.sk, Cancer Research Institute, Bratislava, Slovak Republic; <sup>2</sup>Nutrition Division, Institute of Food Research, Norwich Research Park, Norwich NR4 7UA, UK; <sup>3</sup>School of Medicine, Health Policy and Practice, University of East Anglia, Norwich NR4 7TJ, UK

Received June 8, 2006

The aim of presented study was to further investigate the concentration-dependent changes induced by isothiocyanate iberin (IBN) in human colon carcinoma Caco-2 cells. The concentrations of IBN below IC<sub>50</sub> value (18 µM, 72 h) triggered the augmentation of mRNA levels for phase II detoxification GSTA1 and UGT1A1 enzymes and antioxidant thioredoxin reductase 1 gene in cells treated for 24 h. In addition a significant increase of acetylated H4 histone was detected. The mRNA induction peaked at IC<sub>50</sub> value and returned to level of control cells at 40 µM concentration of IBN. The cell cycle changes, γ-H2AX stainability and the increase of phospho-H3 mitotic marker were induced at concentrations above IC<sub>50</sub> value. Appearance of Annexin V positive apoptotic cells and sub-G1 fragmented DNA as well as decrease of mitochondrial transmembrane potential confirmed cytotoxic effect of IBN observed in MTT assay. The predominance of necrotic cells and profound positivity of γ-H2AX took place at the highest concentration of IBN. Thus, IBN represents the effective member of natural chemopreventive isothiocyanate family with which apoptotic potential can be employed to eliminate tumor cells.

*Key words: iberin, isothiocyanates, phase II enzymes, COX-2, apoptosis, cell cycle, H4 hyperacetylation, γ-H2AX, p-H3 mitotic marker, colon cancer, Caco-2 cell line*

Numerous epidemiological studies indicate that frequent consumption of relatively large amounts of a wide variety of fruits and vegetables have been associated with a reduced incidence of cancer [1, 2]. Especially, cruciferous vegetables such

as broccoli, cabbage, Brussels sprouts and cauliflower contain substantial quantities of glucosinolates, the precursors of the potential cancer-protective isothiocyanates (ITCs) [3].

The considerable portion of the chemopreventive effects of ITCs were attributed to their inhibition of the metabolic carcinogen activation by cytochrome P450s, coupled with strong induction of phase II detoxifying capacity and cellular antioxidant enzymes [4–11]. Data indicate that well-known isothiocyanate SFN possesses anti-inflammatory activity, resulting in down-regulation of LPS-stimulated iNOS, COX-2, and TNF-α expression [12].

The involvement of several mitogenic pathways in ITCs-induced apoptosis have been assumed, e.g., an extracellular signal-regulated kinases ERK1/2 [13], JNK/c-Jun signaling cascade [14, 15] and p38 MAPK [16]. These effects of ITCs on most of the cell signaling cascades are ultimately linked to the growth inhibition and/or apoptotic death of cancer cells [17–19]. Therefore, other different modes of modulation should be taken into account in the cascade of

\*This work was supported in part by EC Marie Curie Training Site Fellowship QLK5-1999-50510, Governmental research and development sub-programme Food quality and safety, No. 2003SP270280E010280E01, and Slovak Grant Agency VEGA No. 2/4069.

\*\*Corresponding author

Abbreviations: IBN – Iberin (1-isothiocyanato-3-(methylsulfanyl)-propane; MAPK – mitogen-activated protein kinase; JNK – c-Jun N-terminal kinase; ERK1/2 – extracellular signal-regulated kinases 1 and 2; ROS – reactive oxygen species; JC-1 – 5,5',6,6'-tetrachloro-1,1',3,3'-tetraethylbenzimidazolylcarbocyanine iodide; FDA – fluorescein diacetate; PI – propidium iodide; MTT – 3-[4, 5-dimethylthiazol-2-yl]-2,5-diphenyl tetrazolium bromide; GST – glutathione S-transferase; UGT – UDP-glucuronosyl-transferase; COX-2 – cyclooxygenase-2; iNOS – inducible nitric oxid synthase; 7-AAD – 7-amino-actinomycin D; TR-1,2 – thioredoxin reductase 1 and 2; HDAC – histone deacetylase;

events leading to cell death, such as induction of caspases [14, 20], mitochondrial death pathway [17, 21], activation of Fas-mediated apoptosis [22] or changes in Bax/Bcl-2 ratio [20]. It has been suggested that oxidative stress by depletion of intracellular glutathione and/or intracellular ROS generation may contribute to signaling events leading to ITCs-induced apoptosis [23, 24].

Growing evidence indicated that ITCs can modulate cell cycle regulatory molecules leading to an accumulation of cells in the G<sub>2</sub>/M phase of the cell cycle [25, 26]. In addition, the inhibition of tubulin polymerization [27], decreased expression of cyclin B1, Cdc25B and Cdc25C, accumulation of inactivated cyclin-dependent kinase 1 [28, 29], and acetylation of histones H3 and H4 [30, 31] were observed.

Our study was focused on the concentration-dependent effects of IBN, an ITC structurally related to SFN, in human colon adenocarcinoma Caco-2 cell line treated for 24 h. In addition to the increase of phase II enzymes mRNA expression, apoptosis induction and the cell cycle deregulation, the decrease of COX-2 mRNA and concentration-dependent acetylation of H4 and phosphorylation of H3 and H2AX histones were found.

## Material and methods

**Reagents.** Iberin (1-isothiocyanato-3-(methylsulfinyl)-propane; IBN) was purchased from LKT Laboratories (St. Paul, MN). Polyclonal rabbit antibodies against phospho-histone H3 (Ser10, mitosis marker p-H3), hyperacetylated histone H4 (hyperAc-H4), mouse monoclonal anti phospho-histone H2AX (Ser139,  $\gamma$ -H2AX) and FITC-conjugated anti-rabbit (mouse) IgG were purchased from Upstate (Lake Placid, NY) and Sigma (Dorset, UK), respectively. Fluorescein diacetate (FDA), dimethyl sulfoxide (DMSO), RNA-se A, propidium iodide (PI), and 3-[4,5-dimethylthiazol-2-yl]-2,5-diphenyl tetrazolium bromide (MTT) were obtained from Sigma (Dorset, UK). Annexin V-PE, JC-1 (5,5',6,6'-tetrachloro-1,1',3,3'-tetraethylbenzimidazolylcarbo-cyanine iodide), and 7-aminoactinomycin D (7-AAD) were purchased from Molecular Probes (Eugene, OR).

**Cell culture and treatment with IBN.** The human colon adenocarcinoma cell line Caco-2 was obtained from the European Collection of Cell Culture (Wiltshire, UK). Stock cells were cultured in RPMI 1640 medium supplemented with 10% fetal calf serum, 100  $\mu$ g/ml penicillin and 50  $\mu$ g/ml streptomycin in humidified air atmosphere with 5% CO<sub>2</sub> at 37 °C. The cultures were maintained for 4–5 days prior to experimental treatment.

The cells were treated on 60-mm dishes when cultures achieved about 50–60% of confluence. Cells were exposed to various concentrations of IBN (stock solution of IBN dissolved in DMSO) for 6 h and 24 h, and an equal volume of DMSO (final concentration <0.1%) was added to the control cells. The floating cells were collected by centrifugation at 700 x g for 3 min, whereas adherent cells were trypsinized

and collected by centrifugation at 700 x g for 3 min. Pooled cells were washed twice with cold PBS.

**Cell survival assay.** The cells (5x10<sup>3</sup> per well in 200  $\mu$ l of medium) were seeded in a 96-well culture plate and left to adhere to the plastic plates to reach 50–60% confluence before they were exposed to different concentrations of IBN. After 24, 48 and 72 h, the cells were incubated with 50  $\mu$ l of MTT (1 mg/ml) and left in the dark at 37 °C for an additional 4 h. Thereafter, medium was removed, the formazan crystals were dissolved in 200  $\mu$ l of DMSO, and the absorbance was measured at 540 and 690 nm in a Multisoft plate system (Labsystems Oy, Finland). The concentration of drug that inhibited cell survival to 50% (IC<sub>50</sub>) was determined by Calcsyn software.

**Annexin V-PE staining.** Approximately 5x10<sup>5</sup> cells were resuspended in 100  $\mu$ l of 1 x binding buffer (10 mM Hepes/NaOH, 140 mM NaCl, 2.5 mM CaCl<sub>2</sub>, pH 7.4) and mixed with 5  $\mu$ l of Annexin V-PE and 5  $\mu$ l of 7-AAD (1 mg/ml stock). After 15 min incubation in the dark at room temperature, the cells were analyzed using a Coulter Epics Altra flow cytometer.

**Fluorescein diacetate (FDA)/PI staining.** Approximately 5x10<sup>5</sup> cells were resuspended in 400  $\mu$ l of PBS/0.2% BSA containing 10 nM of FDA (from a 5 mM stock in DMSO) for 30 min at room temperature. Then cells were cooled and 4  $\mu$ l of PI (1 mg/ml) was added. Finally, after 15 min the stained cells were analyzed using a Coulter Epics Altra flow cytometer.

**Cytofluorimetric analysis of mitochondrial potential.** Approximately 5x10<sup>5</sup> cells were incubated in 400  $\mu$ l of PBS/0.2% BSA containing 4  $\mu$ M of JC-1 (from a 7.7 mM stock in DMSO) for 30 min at 37 °C. After 30 min incubation in the dark at 37 °C, the cells were analyzed using a Coulter Epics Altra flow cytometer.

**Cell cycle analysis.** For flow cytometric analyses of DNA cell cycle profiles, approximately 5x10<sup>5</sup> cells were resuspended in 0.05% Triton X-100 and 15  $\mu$ l of RNA-se A (10 mg/ml) for 20 min at 37 °C. After placing on ice for at least 10 min, PI (50  $\mu$ g/ml) was added. Finally, after 15 min the stained cells were analyzed using a Coulter Epics Altra flow cytometer.

**Detection of histones activation.** For flow cytometric analysis of histones expression, approximately 1x10<sup>6</sup> cells were collected by trypsinization and pooled together with floating cells. The cells were rinsed twice with cold PBS, and fixed in 1% methanol-free paraformaldehyde in PBS at 0 °C for 3 min, washed in PBS/0.2% BSA and then resuspended in 70% ethanol for at least 2 h at –20 °C. The cells were then washed twice in 1% solution of BSA in PBS to suppress non-specific antibody binding. Then the cell pellet was suspended in 100  $\mu$ l of 1% BSA containing 1:200 diluted rabbit p-H3, hyperAc-H4 or mouse  $\gamma$ -H2AX antibodies. Cells were incubated for 1 h at room temperature, washed twice with PBS/1% BSA, and resuspended in 100  $\mu$ l of 1:60 diluted FITC-conjugated anti-rabbit immunoglobulin or FITC-con-

jugated anti-mouse immunoglobulin for 30 min at room temperature in the dark, respectively. After double washing in PBS, cells were counterstained with 5  $\mu\text{g}/\text{ml}$  of PI dissolved in PBS, for 15 min at 4  $^{\circ}\text{C}$ . Cellular fluorescence was measured using a Coulter Epics Altra flow cytometer.

**Flow cytometric measurements and data analysis.** Coulter Epics Altra flow cytometer was equipped with 488 nm excitation laser and fluorescence emission was measured using bandpass filter set 525, 575, 610, 675 nm. Forward/side light scatter characteristic was used to exclude the cell debris from the analysis. For each analysis,  $1 \times 10^4$  cells were acquired for analysis. Data were analyzed with WinMDI version 2.7 software (J. Trotter, Scripps Research Institute, La Jolla, CA). The cell cycle calculations were performed with MULTI-CYCLE Software (Phoenix Flow System).

**Real-time RT-PCR for phase II enzymes and cellular defensive enzymes.** Total RNA from Caco-2 cells was isolated using a GenElute<sup>TM</sup> Total Mammalian RNA kit (Sigma, UK) as specified in the manufacturer's instructions. The RNA concentration and purity were determined by measurement of the absorbance at 260 and 280 nm. The target mRNA was quantified by real-time RT-PCR (TaqMan<sup>®</sup>) using an ABI PRISM<sup>TM</sup> 7700 Sequence Detection System (Applied Biosystems, Warrington, UK). Forward- and reverse primers and the fluorogenic TaqMan<sup>®</sup> probes were designed using ABI PRISM Primer Express Software (Applied Biosystems). Primer and probe sequences for the assays performed were: UGT1A1 forward primer 5'-GGT GAC TGT CCA GGA CCT ATT GA-3', reverse primer 5'-TAG TGG ATT TTG GTG AAG GCA GTT-3', probe 5'-ATT ACC CTA GGC CCA TCA TGC CCA ATA TG-3'; GSTA1 forward primer 5'-CAG CAA GTG CCA ATG GTT GA-3', reverse primer 5'-TAT TTG CTG GCA ATG TAG TTG AGA A-3', probe 5'-TGG TCT GCA CCA GCT TCA TCC CAT C-3'; COX-2 forward primer 5'-GAA TCA TTC ACC AGG CAA ATT G-3', reverse primer 5'-TCT GTA CTG CGG GTG GAA CA-3', probe 5'-TCC TAC CAC CAG CAA CCC TGC CA-3'; TR-1 forward primer 5'-CCA CTG GTG AAA GAC CAC GTT-3', reverse primer 5'-AGG AGA AAA GAT CAT CAC TGC TGA T-3', probe 5'-CAG TAT TCT TTG TCA CCA GGG ATG CCC A-3'; TR-2 forward primer 5'-GCA CCA CCG GCA AGG A-3', reverse primer 5'-CAG CCT TCT CCA AAT TCA GAC TTC-3', probe 5'-CTG TGG GCC ATA GGT CGA GTC CCA-3'. The probes were labeled with a 5' reporter dye FAM (6-carboxyfluorescein) and 3' quencher dye TAMRA (6-carboxytetramethylrhodamine). RT-PCR reactions were carried out in a 96-well plate in a total volume of 25  $\mu\text{l}$  per well consisting of TaqMan<sup>®</sup> one-step RT-PCR master mix reagent (Applied Biosystems), 10 ng of total RNA, 100 nM probe, 200 nM forward primer and 200 nM (300 nM) reverse primer to amplify UGT1A1, TR-2, and GSTA1, (TR-1); or 200 nM probe, 300 nM forward primer and 300 nM reverse primer to amplify COX-2. A reverse transcription was performed for 30 min at 48  $^{\circ}\text{C}$ , then an AmpliTaq<sup>TM</sup> gold activation for 10 min at 95  $^{\circ}\text{C}$ , followed by

40 PCR cycles of denaturation at 95  $^{\circ}\text{C}$  for 15 s and finally annealing/extension at 60  $^{\circ}\text{C}$  for 1 min. Reactions were carried out in triplicate. The data were analyzed by TaqMan<sup>®</sup> software using a standard curve method as described in User Bulletin No. 2 (ABI PRISM<sup>TM</sup> 7700 Sequence Detection System) to quantify the mRNA amount. Standard curves were constructed for each amplified gene sequence using 1, 5, 10, 20 and 40 ng of total RNA per reaction in triplicates. GAPDH was used as an internal reference gene (GAPDH forward primer 5'-GAA GGT GAA GGT CGG AGT C-3', GAPDH reverse primer 5'-GAA GAT GGT GAT GGG ATT TC -3', GAPDH probe 5'-CAA GCT TCC CGT TCT CAG CC -3').

## Results

**Cytotoxic effect of IBN.** MTT assay was employed to assess the cytotoxicity of IBN in Caco-2 cells using six serial two-fold dilutions of IBN started at 160  $\mu\text{M}$  concentration. Figure 1 shows differences of IC<sub>50</sub> values at respective time points achieving IC<sub>50</sub> value of  $18 \pm 1.7$   $\mu\text{M}$  for 72 h treatment. The proliferation of Caco-2 cells was not affected by IBN in the low concentration range (5 and 10  $\mu\text{M}$ ), while the concentrations of IBN above 10  $\mu\text{M}$  reduced significantly the viability of cells in time-dependent manner.

**Dissipation of mitochondrial membrane potential.** The lipophilic dye JC-1 measured alterations in mitochondrial membrane potential were applied to delineate the mechanism of IBN cytotoxicity in the Caco-2 cells (Fig. 2A,D). Cells with normal polarized mitochondrial membranes emit green-orange fluorescence and cells with depolarized mitochondrial membranes emit only green fluorescence. Production of JC-1 monomers is directly correlated to change of mitochondrial membrane potential  $\psi_m$  and its breakdown in dying cells results in increase of green fluorescence. Exposure of Caco-2 cells to the highest concentration (100  $\mu\text{M}$ ,

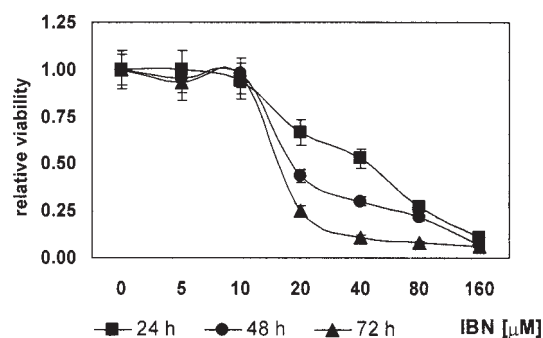


**Figure 1.** Cytotoxic effect of IBN on Caco-2 cells. The Caco-2 cells were treated with various concentrations (5–160  $\mu\text{M}$ ) of IBN for 24, 48 and 72 h in 96 well plates. Each treatment with a specific concentration of a compound was done in quadruplicate. The data presented are representative of three independent experiments and are expressed as mean  $\pm$ SD.

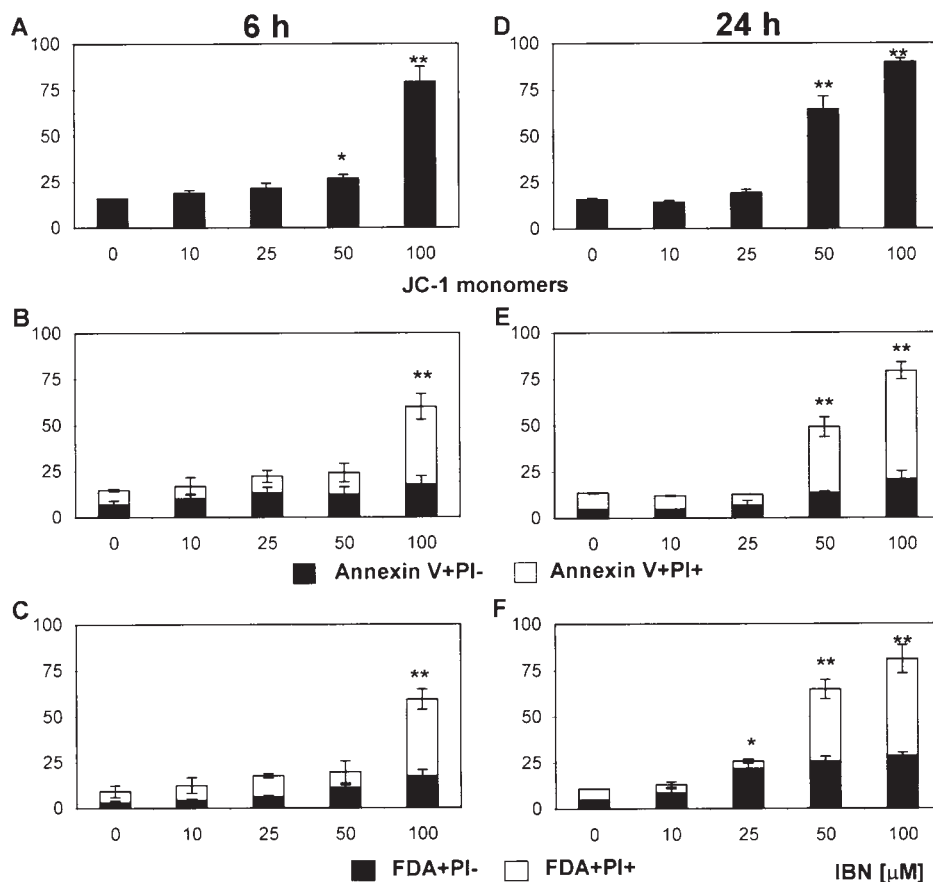


**Figure 2.** Effect of IBN on mitochondrial membranes depolarization (A, D) and apoptosis (B, C, E, F) induction in Caco-2 cells treated for 6 h (A–C) and 24 h (D–F). The cells were exposed to either DMSO (control) cells or IBN (10–100  $\mu$ M), stained with JC-1 dye (A, D), Annexin V/7-AAD (B, E) or FDA/PI (C, F) and analyzed using a Coulter Epics Altra flow cytometer. The data presented are representative of three independent experiments and are expressed as mean  $\pm$ SD. Statistical significance from the controls, \* $p$ <0.05; \*\* $p$ <0.01.

Fig. 2A) of IBN for 6 h resulted in a statistically significant increase of JC-1 monomers. The prolonged 24 h treatment of Caco-2 cells with higher concentrations (50 and 100  $\mu$ M, Fig. 2D) of IBN significantly increased production of JC-1 monomers up to 4- and 6-fold the level in control cells, respectively. These results suggest that mitochondrial membrane potential was reduced significantly by IBN treatment in dose- and time-dependent manner.

**Apoptosis induction by IBN.** Next, we addressed the question whether cytotoxic effect of IBN at least in part correlated with one of the basic characteristic marks of chemoprevention, induction of apoptosis. Flow cytometric Annexin V binding analysis (Fig. 2B,E) of IBN treated cells allows to enumerate cells with phosphatidylserine exposition on the outer surface of cell membrane as a hallmark of early apoptosis and permits the discrimination of apoptotic (Annexin V stained cells without altered membrane permeability) from necrotic cells (with both Annexin V and 7-AAD staining). The control DMSO-treated cells showed around

15% of Annexin V+/7-AAD- and Annexin V+/7-AAD+ double positive cells. Low concentrations of IBN induced gradual nonsignificant increase of apoptotic and necrotic cells. Significant increase of Annexin V+/7-AAD- apoptotic (13%) and Annexin V+/7-AAD+ necrotic cells (35%) in Caco-2 cell line was observed after 24 h treatment with 50  $\mu$ M concentration of IBN. The highest concentration of IBN resulted in a significant increase of Annexin V+/7-AAD- apoptotic cells (18% and 21%) and Annexin V+/7-AAD+ necrotic cells (42% and 59%) after both 6 h and 24 h treatments in comparison with controls (Fig. 2).

Cytofluorometric analysis of FDA/PI staining for detection of viable, apoptotic, and dead cells was performed (Fig. 2C,F). Exposure of cells to 50 or 100  $\mu$ M concentrations of IBN for 6 and 24 h resulted in a gradual increase of FDA-/PI-apoptotic population (11% or 25% and 17% or 28%, respectively). Using FDA/PI staining, a similar percentage of FDA-/PI+ necrotic populations was observed as by using Annexin V/7-AAD staining.

**IBN induces the mRNA expression.** Induction of phase II detoxifying enzymes, one of the characteristic marks of chemoprevention, appears to be of a potential protective mechanism elicited by chemopreventive agents such as ITCs. Caco-2 cells were treated with IBN (5–40  $\mu$ M) for 24 h (Fig. 3). TaqMan<sup>®</sup> real-time-PCR analysis showed that IBN induced the 3.3- and 3.15-fold increase of UGT1A1 and GSTA1 mRNAs at 10 and 20  $\mu$ M concentration of IBN, respectively (Fig. 3A). The amounts of both mRNAs declined to the control level after 40  $\mu$ M IBN treatment, probably due to the cytotoxic effect of IBN as demonstrated in Figure 2. The level of housekeeping gene GAPDH mRNA was unchanged in the whole range of IBN concentrations used. The expression of TR-1 mRNA was up-regulated in treated Caco-2 cells and peaked at 20  $\mu$ M concentration of IBN (Fig. 3B). A slight decrease of TR-2 and COX-2 mRNA levels at 20  $\mu$ M concentration of IBN was observed. In contrast to GST1A, UGT1A1 or TR-1 mRNAs, the highest concentration (40  $\mu$ M) of IBN significantly decreased TR-2 and

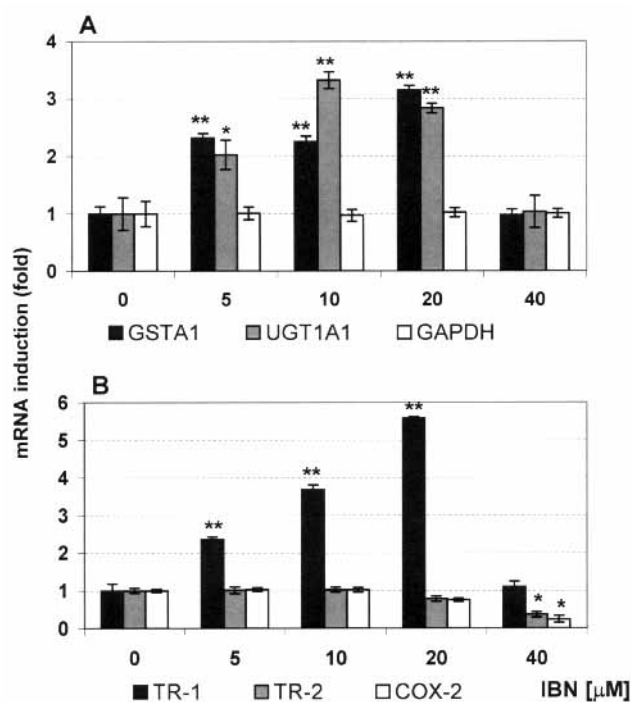


**Figure 3.** Effect of IBN on mRNA transcription. Real-time RT-PCR analysis of mRNA levels of phase II enzymes (GSTA1 and UGT1A1) and cellular defensive enzymes (TR-1, TR-2, COX-2) in Caco-2 cells. Cells were incubated with different concentrations (5, 10, 20 and 40  $\mu$ M) of IBN for 24 h. DMSO was added to the control cells. GAPDH was used as a housekeeping gene. The data presented are average of two experiments each in triplicate, data represent mean  $\pm$ SD. Data were normalized against control=1. Statistical significance from the controls, \* $p$ <0.05; \*\* $p$ <0.01.

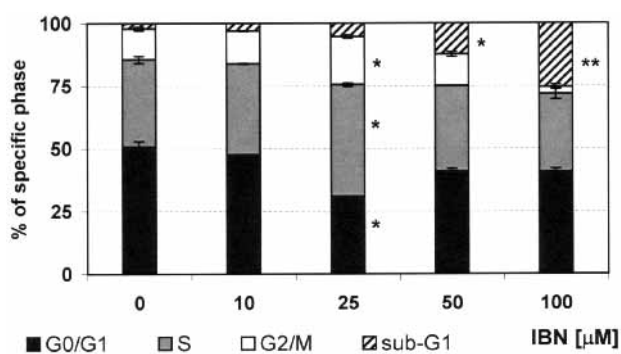


**Figure 4.** Effect of IBN on distribution of different cell cycle phases (G<sub>0</sub>/G<sub>1</sub>, S and G<sub>2</sub>/M) and sub-G<sub>1</sub> phase in Caco-2 cells. After treatment for 24 h, cells were collected, detergent permeabilized and stained with 50  $\mu$ g/ml concentration of PI in the presence of RNA-se A. Percentage of sub-G<sub>1</sub> fraction was obtained from SSC versus log FL2 dot plot analysis using WinMDI software. The distribution of cells in G<sub>0</sub>/G<sub>1</sub>, S and G<sub>2</sub>/M phase was analyzed by Multi-cycle software. Three independent experiments were performed and mean  $\pm$ SD are presented. Statistical significance from the controls, \* $p$ <0.05; \*\* $p$ <0.01.

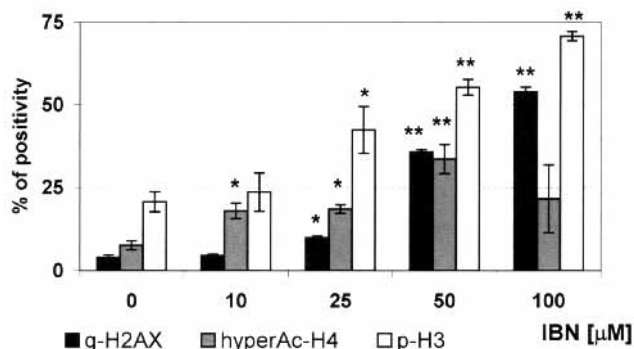


**Figure 5.** Effect of IBN on posttranslational modification of H3, H2AX and H4 histones. The control and IBN-treated Caco-2 cells (10, 25, 50 and 100  $\mu$ M) for 24 h were stained with respective polyclonal antibodies against phosphorylated H3 and H2AX and acetylated H4 histones. Two independent experiments were performed and mean  $\pm$ SD are presented. Statistical significance from the controls, \* $p$ <0.05; \*\* $p$ <0.01.

COX-2 mRNAs expression below the level of untreated control cells. The results show that IBN modulates gene expression of phase II detoxifying enzymes (GSTA1 and UGT1A1) and cellular defensive enzymes (TR-1, TR-2 and COX-2).

*Cell cycle modulation and DNA fragmentation by IBN.* Next, we raised a question of whether IBN induced the cell cycle arrest a frequently observed event in ITCs treated cells. Untreated control cells were primarily in the G<sub>0</sub>/G<sub>1</sub> (51%) and in the S phase (35%), with a small percentage at G<sub>2</sub>/M phase (13%). As can be seen in Figure 4, 24 h exposure of Caco-2 cells to 25  $\mu$ M concentration of IBN resulted in a statistical significant increase of S and G<sub>2</sub>/M fractions that were accompanied by a corresponding decrease in G<sub>0</sub>/G<sub>1</sub> phase of the cell cycle. In addition, a quantification of the proportion of cells with DNA content below that of G<sub>1</sub> cells (sub-G<sub>1</sub> cells, a hallmark of late apoptosis) was performed. At higher IBN concentrations the appearance of apoptotic sub-G<sub>1</sub> cells, at the expense of S and G<sub>2</sub>/M fractions, was observed. As shown in Figure 5, after 24 h of treatment with 50  $\mu$ M and 100  $\mu$ M of IBN, 12 and 25% of sub-G<sub>1</sub> cells were found, respectively. When summarizing, all independent techniques used (Annexin V/7-AAD, FDA/PI, sub-G<sub>1</sub>) clearly indicated that IBN induced apoptotic cell death in colon Caco-2 cells in dose-dependent manner and that apoptosis correlated with dissipation of mitochondrial membrane potential.

*Induction of covalent modification of histone proteins.* Next, we analyzed a possible correlation between IBN-mediated cell cycle arrest and the levels of covalently modified histones in Caco-2 cells. We determined the effect of IBN treatment on the levels of  $\gamma$ -H2AX, a DNA double strand breaks marker, the mitosis marker p-H3, and on the hyperacetylation of histone H4 after 24 h of IBN treatment (Fig. 5). We have observed a significant increase of phosphorylated forms of H3 and H2AX histones started at 25  $\mu$ M concentra-

tion of IBN. As low as 10  $\mu\text{M}$  concentration of IBN was sufficient to increase the hyperacetylation of histone H4, that reached the maximum at 50  $\mu\text{M}$  concentration of IBN. These results suggested that IBN-induced apoptotic death in Caco-2 cells was preceded by the covalent modification of histone proteins.

## Discussion

In the present study we have evaluated the effect of IBN treatment on Caco-2 cells that completes our previous findings obtained with SFN and erucin, the aliphatic ITCs with one methylene group longer chain than in IBN. We have assayed some aspects of natural ITC actions such as growth inhibition, apoptotic cell death, phase II enzymes induction, as well as changes in histone acetylation, phosphorylation and cell cycle alterations.

Considering the  $\text{IC}_{50}$  value IBN belongs to the most cytotoxic aliphatic ITCs tested in Caco-2 cells (50, 23, and 21  $\mu\text{M}$  for AITC, SFN, and erucin, respectively) [25, 32]. The induction of apoptosis within relatively narrow concentration window is often observed in ITCs treated cells [33]. In accordance with our previous study a gradual concentration-dependent increase of apoptotic Caco-2 cells was observed. Similarly, treated cells exhibited the significant increase of necrotic cells primarily at higher concentrations of IBN used. The sharp increase in both apoptotic and necrotic cells was accompanied by a clear dissipation of mitochondrial transmembrane potential represented by accumulation of JC-1 monomers.

Recently, the mitochondrion was proposed to be a primary target in ITCs-induced growth inhibition and apoptosis, linked with the early ROS generation, alteration of cellular redox state [8, 24, 34], and modulation of select Bcl-2 family members [35]. It was shown, that alteration in intracellular redox status may be one means by which SFN acts to increase phase 2 enzymes expression [6]. We have found that IBN treatment induced also the known set of gene expression alterations caused by others ITCs [6, 8, 36]. As low as 5  $\mu\text{M}$  concentration of IBN induced UGT1A1 and GSTA1 mRNA of phase II enzymes, as well as TR-1 mRNA linked with cellular redox modulation. In the earlier reports corresponding interaction of SFN with glutathione and other redox regulators like thioredoxin and Ref-1 was found [12, 34, 37]. This low concentration effect of IBN may represent the cell response aimed at regulation of redox-sensitive "sulphydryl switches", linked partially with nuclear translocation of proteins [34, 38, 39]. The IBN-induced decrease of COX-2 mRNA expression is consistent with modulation of RNA polymerase II elongation by HDAC inhibitors [40, 41]. In addition, inhibitors of COX-2 as well as SFN itself sensitized tumor cells to TRAIL-induced apoptosis [42–44]. Then sustained acetylation of H4 histone and decrease of COX-2 mRNA observed in our study might represent a possible histone deacetylase inhibitory activity of IBN.

Effect of equimolar concentrations of IBN exerted a significant difference in respect to the extent of apoptotic and necrotic cells induction in comparison with that in SFN and erucin treated cells [32]. There was not a profound  $\text{G}_2/\text{M}$  arrest observed in IBN treated cells as we had seen in SFN and erucin treatment, but an evident cell cycle perturbation unequivocally preceded both the increase of apoptotic and necrotic cell number and the decrease of mitochondrial potential. Recently, the detection of H2AX phosphorylation has emerged as reporter of DNA double strand induction. [45]. Both, the appearance of significant  $\gamma\text{-H2AX}$  staining and cell cycle perturbation have occurred at the same 25  $\mu\text{M}$  concentration of IBN. Such a  $\gamma\text{-H2AX}$  staining in ITCs treated cells is in agreement with our results [46] and those of others [28]. Whether detection of  $\gamma\text{-H2AX}$  represents DNA double strand breaks or the indication of stalled or broken replication forks in S phase [47] is the topic of future investigation.

Increased acetylation of histones was observed in mouse erythroleukemia cells [30] and in human colorectal carcinoma cells treated with allyl-ITC and SFN [31]. We have proved that IBN induced significant hyperacetylation at low concentration (10  $\mu\text{M}$ ) that had no effect on apoptosis induction and modulation of cell cycle. The expression of phosphorylated H3 histone, a mitotic marker, was the third histone modification analyzed in IBN treated Caco-2 cells. The proportion of pH3 in  $\text{G}_2/\text{M}$  cell cycle phase increased in concentration-dependent manner. Taking into account the progressive concentration-dependent decrease of  $\text{G}_2/\text{M}$  cells (Fig. 4) one could speculate, that increase of pH3 proportion is due to preferential elimination of pH3 negative cells from  $\text{G}_2/\text{M}$  fraction as was observed earlier [25]. This is supported by the observation, that apoptosis in synchronized cell culture is generated after complete transition through S phase of the cell cycle [manuscript submitted].

The chemopreventive effect of IBN like other ITCs may be caused by the induction of phase II enzymes, implicated in the detoxification of many carcinogens, thereby protecting cells against DNA damage and subsequent malignant transformation. The known upregulation of p53 and p21 proteins expression by ITCs [46, 48] may lead to reduction of mutation load in error-prone DNA repair [49]. Similarly induction of H4 hyperacetylation is associated with protection of tumor suppressor genes from being transcriptionally repressed in normal cells [50]. Thus, the members of dietary HDAC inhibitor family, IBN and others ITCs can be used to regulate expression of genes involved in cell growth and apoptosis.

We would also like to thank Mr. G PLUMB, Mrs. M. SULIKOVA and Mrs. J. CHOVANCOVA for technical assistance and Mr. J. BACON for TaqMan<sup>R</sup> assays.

## References

- [1] BLOCK G, PATTERSON B, SUBAR A. Fruit, vegetables, and cancer prevention: a review of the epidemiological evidence. *Nutr Cancer* 1992; 18: 1–29.

- [2] STEINMETZ KA, POTTER JD. Vegetables, fruit, and cancer prevention: a review. *J Am Diet Assoc* 1996; 96: 1027–1039.
- [3] VERHOEVEN DT, GOLDBOHRM RA, VAN POPPEL G et al. Epidemiological studies on brassica vegetables and cancer risk. *Cancer Epidemiol Biomarkers Prev* 1996; 5: 733–748.
- [4] BARCELO S, GARDINER JM, GESCHER A et al. CYP2E1-mediated mechanism of anti-genotoxicity of the broccoli constituent sulforaphane. *Carcinogenesis* 1996; 17: 277–282.
- [5] FAULKNER K, MITHEN R, WILLIAMSON G. Selective increase of the potential anticarcinogen 4-methylsulphinylbutyl glucosinolate in broccoli. *Carcinogenesis* 1998; 19: 605–609.
- [6] BROOKS JD, PATON VG, VIDANES G. Potent induction of phase 2 enzymes in human prostate cells by sulforaphane. *Cancer Epidemiol Biomarkers Prev* 2001; 10: 949–954.
- [7] KEUM YS, OWUOR ED, KIM BR et al. Involvement of Nrf2 and JNK1 in the activation of antioxidant responsive element (ARE) by chemopreventive agent phenethyl isothiocyanate (PEITC). *Pharm Res* 2003; 20: 1351–1356.
- [8] NAKAMURA Y, OHIGASHI H, MASUDA S et al. Redox regulation of glutathione S-transferase induction by benzyl isothiocyanate: correlation of enzyme induction with the formation of reactive oxygen intermediates. *Cancer Res* 2000; 60: 219–225.
- [9] ROSE P, FAULKNER K, WILLIAMSON G et al. 7-Methylsulfinylheptyl and 8-methylsulfinyloctyl isothiocyanates from watercress are potent inducers of phase II enzymes. *Carcinogenesis* 2000; 21: 1983–1988.
- [10] MORIMITSU Y, NAKAGAWA Y, HAYASHI K et al. A sulforaphane analogue that potently activates the Nrf2-dependent detoxification pathway. *J Biol Chem* 2002; 277: 3456–3463.
- [11] THIMMULAPPA RK, MAI KH, SRISUMA S et al. Identification of Nrf2-regulated genes induced by the chemopreventive agent sulforaphane by oligonucleotide microarray. *Cancer Res* 2002; 62: 5196–5203.
- [12] HEISS E, HERHAUS C, KLIMO K et al. Nuclear factor kappa B is a molecular target for sulforaphane-mediated anti-inflammatory mechanisms. *J Biol Chem* 2001; 276: 32008–32015.
- [13] YUR, LEI W, MANDLEKAR S et al. Role of a mitogen-activated protein kinase pathway in the induction of phase II detoxifying enzymes by chemicals. *J Biol Chem* 1999; 274: 27545–27552.
- [14] XU K, THORNALLEY PJ. Signal transduction activated by the cancer chemopreventive isothiocyanates: cleavage of BID protein, tyrosine phosphorylation and activation of JNK. *Br J Cancer* 2001; 84: 670–673.
- [15] YUR, JIAO JJ, DUH JL et al. Phenethyl isothiocyanate, a natural chemopreventive agent, activates c-Jun N-terminal kinase 1. *Cancer Res* 1996; 56: 2954–2959.
- [16] XIAO D, SINGH SV. Phenethyl isothiocyanate-induced apoptosis in p53-deficient PC-3 human prostate cancer cell line is mediated by extracellular signal-regulated kinases. *Cancer Res* 2002; 62: 3615–3619.
- [17] GAMET-PAYRASTRE L, LI P, LUMEAU S et al. Sulforaphane, a naturally occurring isothiocyanate, induces cell cycle arrest and apoptosis in HT29 human colon cancer cells. *Cancer Res* 2000; 60: 1426–1433.
- [18] BONNESEN C, EGGLESTON IM, HAYES JD. Dietary indoles and isothiocyanates that are generated from cruciferous vegetables can both stimulate apoptosis and confer protection against DNA damage in human colon cell lines. *Cancer Res* 2001; 61: 6120–6130.
- [19] FIMOGNARI C, NUSSE M, CESARI R et al. Growth inhibition, cell-cycle arrest and apoptosis in human T-cell leukemia by the isothiocyanate sulforaphane. *Carcinogenesis* 2002; 23: 581–586.
- [20] SINGH AV, XIAO D, LEW KL et al. Sulforaphane induces caspase-mediated apoptosis in cultured PC-3 human prostate cancer cells and retards growth of PC-3 xenografts in vivo. *Carcinogenesis* 2004; 25: 83–90.
- [21] NAKAMURA Y, KAWAKAMI M, YOSHIHIRO A et al. Involvement of the mitochondrial death pathway in chemopreventive benzyl isothiocyanate-induced apoptosis. *J Biol Chem* 2002; 277: 8492–8499.
- [22] PULLAR JM, THOMSON SJ, KING MJ et al. The chemopreventive agent phenethyl isothiocyanate sensitizes cells to Fas-mediated apoptosis. *Carcinogenesis* 2004; 25: 765–772.
- [23] KIM BR, HU R, KEUM YS et al. Effects of glutathione on antioxidant response element-mediated gene expression and apoptosis elicited by sulforaphane. *Cancer Res* 2003; 63: 7520–7525.
- [24] SINGH SV, SRIVASTAVA SK, CHOI S et al. Sulforaphane-induced cell death in human prostate cancer cells is initiated by reactive oxygen species. *J Biol Chem* 2005; 280: 19911–19924.
- [25] JAKUBIKOVA J, SEDLAK J, BACON J et al. Effects of MEK1 and PI3K inhibitors on allyl-, benzyl- and phenylethyl-isothiocyanate-induced G2/M arrest and cell death in Caco-2 cells. *Int J Oncol* 2005; 27: 1449–1458.
- [26] SRIVASTAVA SK, XIAO D, LEW KL et al. Allyl isothiocyanate, a constituent of cruciferous vegetables, inhibits growth of PC-3 human prostate cancer xenografts in vivo. *Carcinogenesis* 2003; 24: 1665–1670.
- [27] JACKSON SJ, SINGLETARY KW. Sulforaphane: a naturally occurring mammary carcinoma mitotic inhibitor, which disrupts tubulin polymerization. *Carcinogenesis* 2004; 25: 219–227.
- [28] SINGH SV, HERMAN-ANTOSIEWICZ A, SINGH AV et al. Sulforaphane-induced G2/M phase cell cycle arrest involves checkpoint kinase 2-mediated phosphorylation of cell division cycle 25C. *J Biol Chem* 2004; 279: 25813–25822.
- [29] XIAO D, SRIVASTAVA SK, LEW KL et al. Allyl isothiocyanate, a constituent of cruciferous vegetables, inhibits proliferation of human prostate cancer cells by causing G2/M arrest and inducing apoptosis. *Carcinogenesis* 2003; 24: 891–897.
- [30] LEA MA, RANDOLPH VM, LEE JE et al. Induction of histone acetylation in mouse erythroleukemia cells by some organosulfur compounds including allyl isothiocyanate. *Int J Cancer* 2001; 92: 784–789.
- [31] MYZAK MC, KARPLUS PA, CHUNG FL et al. A novel mechanism of chemoprotection by sulforaphane: inhibition of histone deacetylase. *Cancer Res* 2004; 64: 5767–5774.
- [32] JAKUBIKOVA J, SEDLAK J, MITHEN R et al. Role of PI3K/Akt and MEK/ERK signaling pathways in sulforaphane- and erucin-induced phase II enzymes and MRP2 transcription, G2/M arrest and cell death in Caco-2 cells. *Biochem Pharmacol* 2005; 69: 1543–1552.

- [33] KUANG YF, CHEN YH. Induction of apoptosis in a non-small cell human lung cancer cell line by isothiocyanates is associated with P53 and P21. *Food Chem Toxicol* 2004; 42: 1711–1718.
- [34] JAKUBIKOVA J, SEDLAK J, BODO J et al. Effect of isothiocyanates on nuclear accumulation of NF-kappaB, Nrf2, and thioredoxin in Caco-2 cells. *J Agric Food Chem* 2006; 54: 1656–1662.
- [35] TANG L, ZHANG Y. Mitochondria are the primary target in isothiocyanate-induced apoptosis in human bladder cancer cells. *Mol Cancer Ther* 2005; 4: 1250–1259.
- [36] SVEHLIKOVA V, WANG S, JAKUBIKOVA J et al. Interactions between sulforaphane and apigenin in the induction of UGT1A1 and GSTA1 in CaCo-2 cells. *Carcinogenesis* 2004; 25: 1629–1637.
- [37] WANG W, WANG S, HOWIE AF et al. Sulforaphane, erucin, and iberin up-regulate thioredoxin reductase 1 expression in human MCF-7 cells. *J Agric Food Chem* 2005; 53: 1417–1421.
- [38] HEISS E, GERHAUSER C. Time-dependent modulation of thioredoxin reductase activity might contribute to sulforaphane-mediated inhibition of NF-kappaB binding to DNA. *Antioxid Redox Signal* 2005; 7: 1601–1611.
- [39] JAKUBIKOVA J, SEDLAK J. Garlic-derived organosulfides induce cytotoxicity, apoptosis, cell cycle arrest and oxidative stress in human colon carcinoma cell lines. *Neoplasma* 2006; 53: 191–199.
- [40] TONG X, YIN L, JOSHI S et al. Cyclooxygenase-2 regulation in colon cancer cells: modulation of RNA polymerase II elongation by histone deacetylase inhibitors. *J Biol Chem* 2005; 280: 15503–15509.
- [41] MYZAK MC, HARDIN K, WANG R et al. Sulforaphane inhibits histone deacetylase activity in BPH-1, LnCaP and PC-3 prostate epithelial cells. *Carcinogenesis* 2006; 27: 811–819.
- [42] MARTIN S, PHILLIPS DC, SZEKELY-SZUCS K et al. Cyclooxygenase-2 inhibition sensitizes human colon carcinoma cells to TRAIL-induced apoptosis through clustering of DR5 and concentrating death-inducing signaling complex components into ceramide-enriched caveolae. *Cancer Res* 2005; 65: 11447–11458.
- [43] MATSUI TA, SOWA Y, YOSHIDA T et al. Sulforaphane enhances TRAIL-induced apoptosis through the induction of DR5 expression in human osteosarcoma cells. *Carcinogenesis* 2006; 27: 1768–1777.
- [44] KIM H, KIM EH, EOM YW et al. Sulforaphane sensitizes tumor necrosis factor-related apoptosis-inducing ligand (TRAIL)-resistant hepatoma cells to TRAIL-induced apoptosis through reactive oxygen species-mediated up-regulation of DR5. *Cancer Res* 2006; 66: 1740–1750.
- [45] ROGAKOU EP, PILCH DR, ORR AH et al. DNA double-stranded breaks induce histone H2AX phosphorylation on serine 139. *J Biol Chem* 1998; 273: 5858–5868.
- [46] BODO J, JAKUBIKOVA J, CHALUPA I et al. Apoptotic effect of ethyl-4-isothiocyanatobutanoate is associated with DNA damage, proteasomal activity and induction of p53 and p21(cip1/waf1). *Apoptosis* 2006; 11(8): 1299–1310.
- [47] MACPHAIL SH, BANATH JP, YU Y et al. Cell cycle-dependent expression of phosphorylated histone H2AX: reduced expression in unirradiated but not X-irradiated G1-phase cells. *Radiat Res* 2003; 159: 759–767.
- [48] MYZAK MC, DASHWOOD WM, ORNER GA et al. Sulforaphane inhibits histone deacetylase in vivo and suppresses tumorigenesis in Apc-minus mice. *FASEB J* 2006; 20: 506–508.
- [49] AVKIN S, SEVILYA Z, TOUBE L et al. p53 and p21 Regulate error-prone DNA repair to yield a lower mutation load. *Mol Cell* 2006; 22: 407–413.
- [50] SHIA WJ, PATTENDEN SG, WORKMAN JL. Histone H4 lysine 16 acetylation breaks the genome's silence. *Genome Biol* 2006; 7: 217.